

[18F]-PSMA-1007-PET for evaluation of kidney function

Philipp Rassek (✉ philipp.rassek@ukmuenster.de)

University Hospital Muenster <https://orcid.org/0000-0003-0838-6019>

Michael Schäfers

University Hospital Muenster

Kambiz Rahbar

University Hospital Muenster

Philipp Backhaus

University Hospital Muenster

Research Article

Keywords: PSMA, PET, kidney function, renal scintigraphy

Posted Date: October 25th, 2022

DOI: <https://doi.org/10.21203/rs.3.rs-2183068/v1>

License: © ⓘ This work is licensed under a Creative Commons Attribution 4.0 International License.

[Read Full License](#)

Abstract

Purpose

Prostate-specific membrane antigen (PSMA) is present in the proximal tubule cells of the kidneys. This results in high renal tracer uptake in PSMA-PET, which may contain useful information on renal function. As part of the clinical evaluation for [^{177}Lu]-PSMA therapies, patients undergo PSMA-PET and often additional [$^{99\text{m}}\text{Tc}$]-mercapto-acetyltriglycine (MAG3) scintigraphy to assess renal function. Aim of this study was to evaluate estimation of renal function with [^{18}F]-PSMA-1007-PET/CT (PSMA-PET) by comparison to synchronous MAG3-scintigraphies.

Methods

We retrospectively investigated 73 prostate cancer patients with 93 synchronously available PSMA-PET/CT, MAG3-scintigraphies and serum creatinine. For determination of split renal function in PSMA-PET/CT, we evaluated the relative unilateral total renal PSMA uptake, i.e. SUV_{mean} multiplied by the renal volume ($\text{SRF}_{\text{PSMA-TOTAL}}$) and relative unilateral maximal standardized uptake value (SRF_{SUV}). These were compared to MAG3 split renal function (SRF_{MAG3}) using Pearson correlation and receiver operating characteristics analysis. For determination of global renal function, correlation of bilateral total renal PSMA uptake with MAG3 tubular excretion rate and serum creatinine was assessed.

Results

SRF_{MAG3} was strongly correlated with $\text{SRF}_{\text{PSMA-TOTAL}}$ ($r=0.872$, $p<0.001$) and with SRF_{SUV} ($r=0.815$, $p<0.001$). Relevant abnormalities of SRF_{MAG3} (unilateral renal function $< 25\%$) could be detected with sensitivities and specificities of 90% and 92% for $\text{SRF}_{\text{PSMA-TOTAL}}$, and 80% and 95% for SRF_{SUV} . Measures of absolute renal function were only weakly correlated with bilateral total renal PSMA uptake.

Conclusion

Renal [^{18}F]-PSMA-1007 uptake allowed to quantify renal split function with good accuracy based on $\text{SRF}_{\text{PSMA-TOTAL}}$ or SRF_{SUV} .

Background

In recent years, the prostate-specific membrane antigen (PSMA) obtained a dominant role as a molecular target structure for PET imaging and radioligand therapies in prostate cancer [1]. PSMA is a transmembrane protein overexpressed on the surface of prostate cancer cells, though not as exclusively as its name would suggest [2]. Physiologic PSMA expression is therefore also found in different tissues; in the kidneys PSMA expression has been immunohistochemically confirmed in a subset of renal proximal tubule cells [3]. The resulting specific binding of PSMA radioligands to the kidneys goes along with significant organ doses that are potentially relevant for [^{177}Lu]-PSMA therapies [4].

Although specific tracer uptake in the kidneys is principally an undesired feature in PSMA-directed molecular imaging and therapy, it could be rendered useful by extracting relevant information on kidney function from PSMA-PET. Notably, the proximal tubule cells as the cellular source of renal PSMA expression can be considered the primary target of injury and progression of kidney disease [5] establishing a rationale to hypothesize PSMA uptake as a meaningful molecular readout of kidney function. ^{177}Lu -PSMA therapy exposes the kidneys to relevant radiation doses adding to other sources of potential kidney dysfunction in advanced prostate cancer, particularly urinary obstruction induced by local relapse or nodal metastases. Accordingly, kidney function is one of the central limiting factors for initiation and maintenance of PSMA radioligand therapies [6] and requires defined monitoring strategies. In many centres, this is met by performing routine renal scintigraphy with [$^{99\text{m}}\text{Tc}$]-labelled mercapto-acetyl-triglycin (MAG3) [7, 8] to evaluate split and global renal function and to rule out obstruction. According to European guidelines, this is considered optional, whereas PSMA-PET is mandatory in evaluating [^{177}Lu]-PSMA treatment [6]. Thus, the concept of extracting relevant features of renal function from PSMA-PET appears attractive in cases where MAG3-scintigraphy is not available or to even substitute MAG3-scintigraphies.

First evidence for this concept was recently provided in a cohort of 97 patients where split renal function derived from [^{68}Ga]-PSMA-11 uptake was correlated with [$^{99\text{m}}\text{Tc}$]-MAG3-scintigraphies [9]. However, [^{68}Ga]-PSMA-11 might not depict an ideal tracer for this endeavour as the dominant renal excretion of the tracer leads to a renal signal that is composed of excreted and specifically bound tracer. In contrast, the ^{18}F -labelled radiotracer [^{18}F]-PSMA-1007 is not excreted by the kidneys and therefore the renal signal should dominantly derive from tracer bound in the renal cortex. In a recent study, the utility of [^{18}F]-PSMA-1007 to substitute for renal scintigraphy was evaluated based on measurements of different time points and simulated dose reductions in a cohort of 12 patients with predominantly healthy kidneys [10].

In this study, we address the so far lacking insight into the capability of [^{18}F]-PSMA-1007-PET (PSMA-PET) to diagnose relevant abnormalities of split and global renal function. To this end, we compared different measures of PSMA uptake to the results of MAG3-scintigraphies and blood-derived creatinine levels.

Methods

Patient characteristics

Patients with advanced metastasized castration resistant prostate cancer (mCRPC) were included in this retrospective study. Patients gave written informed consent for PSMA-PET/CT and [$^{99\text{m}}\text{Tc}$]-MAG3-scintigraphy as part of their clinical work-up for PSMA radioligand therapy at the department of Nuclear Medicine, University Hospital Muenster, Germany. The local ethics committee approved retrospective scientific analysis. All patients evaluated for radioligand therapy between November 2017 and October 2020 and receiving scans with PSMA-PET and [$^{99\text{m}}\text{Tc}$]-MAG3-scintigraphy in a maximum interval of 30 d

were included. No systematic or random exclusion was applied. An overview of patient characteristics is given in Table 1.

[¹⁸F]-PSMA-1007-PET/CT

According to a one-step procedure by Cardinale et al. described previously [11], [¹⁸F]-PSMA-1007 was produced in a GE Tracer Lab MX synthesizer (GE healthcare, Chalfont St Giles, UK) using a cassette with automatic production sequence obtained from ABX GmbH (Radeberg, Germany). Radiochemical purity was checked by high-performance liquid chromatography. 4 MBq per kg body weight with a maximum of 410 MBq was injected intravenously. A whole-body PSMA-PET/CT from the vertex to distal thighs was performed ~ 120 min after injection. Patients were asked to void before scanning. Imaging was done with a continuous motion scan at 1,5mm/s for lower extremities, 0,8mm/s for hip and 1,1 mm/s for the trunk on a Siemens Biograph mCT scanner (Siemens Healthineers, Erlangen, Germany). A low dose CT was performed for attenuation correction. Standardized uptake values (SUVs) of the kidneys were calculated from ellipsoid volumes of interest (VOIs) covering solely the kidneys using syngo.via software (Siemens Healthineers, Erlangen, Germany). A 30% of SUV_{max} threshold was chosen for calculation of SUV_{mean} and volume, because resulting volumes best matched normal kidney volumes in literature [12–14]).

Determination of split renal function (SRF) from PSMA-PET was attempted by two approaches. First, left SRF_{PSMA-TOTAL} was calculated considering threshold-based kidney volume and SUV_{mean}:

$$SRF_{PSMA-TOTAL} = \frac{(\text{left volume} \times \text{left } SUV_{mean})}{(\text{left volume} \times \text{left } SUV_{mean} + \text{right volume} \times \text{right } SUV_{mean})}$$

Secondly, left SRF_{PSMA-SUV} was calculated based on threshold-based SUV_{max}:

$$SRF_{SUV} = \frac{\text{left } SUV_{max}}{(\text{left } SUV_{max} + \text{right } SUV_{max})}$$

Bilateral total renal PSMA uptake (TRU) for assessing global renal function was calculated as:

$$TRU = \text{left volume} \times \text{left } SUV_{mean} + \text{right volume} \times \text{right } SUV_{mean}$$

[^{99m}Tc]-MAG3-scintigraphy

[^{99m}Tc]-MAG3 was prepared by use of a commercial MAG3 kit (ROTOP® Pharmaka GmbH, Germany) and radiochemical purity of ≥ 94% was verified by elution using a commercial Sep-Pak® Plus C18 cartridge. Examination was performed starting with intravenous injection of a standard activity of 100 MBq [^{99m}Tc]-MAG3. 20 mg of furosemide was typically injected 10 min p.i.. Data acquisition was performed with single photon emission computed tomography/computed tomography (SPECT/CT) cameras, either Siemens Symbia (Siemens Healthineers, Germany) or GE discovery (GE Healthcare, UK). Blood sampling for calculation of tubular extraction rate (TER-MAG3) was performed at baseline, 20 and

28 min p.i. and TER-MAG3 was calculated according to Bubeck [15, 16] (T = Time of blood sample min p.i.; ID = injected activity, cn = normed concentration in plasma at time t (kBq/ml/1.73qm)):

$$TER - MAG3 = A + B \ln \left(\frac{ID}{cn} \right); A = -517 \exp(-0.011xt); B = 295 \exp(-0.016xt)$$

Image acquisition was performed with low-energy-high-resolution collimator, 180 frames à 1 sec, 54 frames à 30 sec, 64x64matrix with patients lying on the scanner table and detector position from posterior; patients with ureteral stents received scintigraphy in upright position standing or sitting to ensure anterograde urinary tracer transport.

Split renal function (SRF) was calculated after defining regions of interest (ROIs) of kidneys using semi-automated software by the camera vendors analysing the renal perfusion phase 60–120 sec p.i. by a slope method [17].

Creatinine values were measured in serum blood samples at the day of the MAG3-scintigraphy.

Statistical analysis

Statistical analysis was done with SPSS Statistics 27 (IBM Inc. Armonk, NY, USA). Strength of correlation between the different measurement methods of renal function was investigated by use of Pearson's correlation. Statistically significant results were defined as a two-sided p-value < 0.05 in Pearson correlation.

Receiver operating characteristics (ROC) analysis with binary classification was applied to analyse the diagnostic performance of PSMA-derived SRF. A maximum Youden index was used for defining ideal thresholds with maximized sensitivity and specificity for PSMA-derived SRFs to predict defined TER-MAG3 abnormalities: $J = \text{sensitivity} + \text{specificity} - 1$

Results

Patient characteristics:

A total of 93 paired PSMA-PET and MAG3-scintigraphies were analysed in 73 patients. Patient characteristics are detailed in Table 1.

Table 1
Patient characteristics.

Characteristics	Mean ± sd (range)
Number of patients	73
Number of paired scans	93
Age	75 ± 8 years
Administered activity [^{99m} Tc]-MAG3	103 ± 6 MBq
Administered activity [¹⁸ F]-PSMA	299 ± 56 MBq
Tubular extraction rate of MAG3 (TER-MAG)	234 ± 48 ml/min/1,73m ² Body surface area (BSA) (107–369)
Creatinine	0.90 ± 32 mg/dl (0.4–2.4)
Split renal function left (MAG3-scintigraphy)	50 ± 14% (0-100%)

Renal split function

SRF_{MAG3} showed a highly significant correlation with SRF_{PSMA-TOTAL} ($r = 0.872$, $p < 0.001$, Fig. 1A) and SRF_{SUV} ($r = 0.815$, $p < 0.001$, Fig. 1B). Consequently, SRF_{PSMA-TOTAL} and SRF_{SUV} were also strongly correlated with each other ($r = 0.824$, $p < 0.001$). Figure 2 shows images and analyses of two representative cases with symmetric versus abnormal SRF_{MAG3} reflected by SRF_{PSMA-TOTAL} and SRF_{SUV}.

The diagnostic performance of PSMA-based determination of any significant abnormal (defined as a unilateral split function $< 40\%$) or highly abnormal split renal function (defined as unilateral split function $< 25\%$) was determined using receiver operating characteristics analyses.

The best threshold for SRF_{PSMA-TOTAL} to detect any significant abnormal split function was 40.5%, resulting in an area under curve (AUC) of 0.79, and a sensitivity of 71% and specificity of 90%. For highly abnormal split function, best threshold for SRF_{PSMA-TOTAL} was 39.5% with AUC of 0.90, and sensitivity of 90% and specificity of 92%, respectively (Fig. 3A, C).

Corresponding values for SRF_{SUV} for a any significant abnormal split function was 46.5%, resulting in AUC of 0.85, sensitivity of 64% and specificity of 90%. For highly abnormal split function, best threshold for SRF_{SUV} was 45.5% resulting in AUC of 0.94, sensitivity of 80% and specificity of 95% (Fig. 3B, D)

Absolute renal function

Bilateral total renal PSMA uptake was weakly inversely correlated with serum creatinine ($r = -0.220$ and $p = 0.034$) (Fig. 4) and weakly correlated with TER-MAG3 ($r = 0.302$ and $p = 0.003$).

To evaluate the potential of PSMA-based measures of absolute renal uptake and to monitor changes of renal function over time, we screened our cohort for patients with significant changes of absolute renal function over time with available MAG3-scintigraphies and PSMA-PET at multiple time points. The concordant course of uptake in few example patients pointed towards a relevance of changes over time in individual patients (Fig. 5), but the number of patients that fulfilled these criteria was not sufficiently high to establish a statistical proof.

Discussion

This retrospective study is first to evaluate the utility of the radiotracer [^{18}F]-PSMA-1007-PET to assess renal split and absolute function in a larger cohort of patients by comparison to [$^{99\text{m}}\text{Tc}$]-MAG3-scintigraphy. We observed a strong correlation of different measures of renal [^{18}F]-PSMA-1007 uptake with MAG3-derived split renal function, but poor correlation with absolute renal function.

Determination of $\text{SRF}_{\text{PSMA-TOTAL}}$ was based on a sophisticated threshold VOI-based technique mirroring the approach and results of a recent study using the tracer [^{68}Ga]-PSMA-11 [18]. The in comparison to [^{68}Ga]-PSMA-11 much lesser excretion of [^{18}F]-PSMA-1007 into urine allowed to omit a cumbersome manual exclusion of the collecting duct system and to use relative unilateral SUV_{max} as a more readily applicable measure of split renal uptake (SRF_{SUV}). Indeed, SUV_{max} based SRF_{SUV} demonstrated a good correlation with MAG3-based split renal function comparable with that of $\text{SRF}_{\text{PSMA-TOTAL}}$. To test the clinical applicability in individual patients, we assessed the diagnostic performance of PSMA-PET to detect abnormalities of split function based on ROC analyses. Particularly for significant abnormalities of split function (> 25%) we found clinically relevant sensitivities and specificities, that were only slightly worse for SRF_{SUV} compared to $\text{SRF}_{\text{PSMA-TOTAL}}$.

The prospect to detect changes of absolute renal function based on bilateral total PSMA uptake is not as clear, as the expression of PSMA in proximal tubule cells may likely vary between patients independent of kidney function and the relationship of absolute tracer uptake and PSMA expression is likely confounded multifactorially, amongst others by the sink effect [19]. Nonetheless, we observed a significant correlation between total PSMA uptake values and measures of absolute renal function, but the relationship was not strong enough to allow to e.g. detect relevant renal insufficiency based on PSMA imaging. This may be more promising and clinically relevant when following-up absolute renal PSMA uptake over time in individual patients. However, our study sample did not feature enough patients with evaluable follow-up and relevant decline of renal function and our evidence therefore remains anecdotal.

A recent study demonstrated the feasibility of [^{18}F]-PSMA-1007 PET to substitute renocortical [$^{99\text{m}}\text{Tc}$]-DMSA-scintigraphy which renal PSMA radiotracer uptake probably most closely corresponds to [10]. In contrast to [$^{99\text{m}}\text{Tc}$]-DMSA, [$^{99\text{m}}\text{Tc}$]-MAG3-scintigraphy plays an important clinical role in adult patients and provides in addition to split renal function valuable information on absolute function (TER-MAG3) and possible obstruction, which is particularly relevant in prostate cancer patients. Based on our data,

[¹⁸F]-PSMA-1007-PET can probably not fully substitute a [^{99m}Tc]-MAG3 scintigraphy that is indicated for evaluating suspected renal disease in individual patients. However, we postulate that the following insights from our study should be considered by [¹⁸F]-PSMA-1007 PET readers as a useful, readily measurable basis for interpreting abnormalities of renal PSMA uptake: (1) A high asymmetry of split renal uptake (SUV_{max} or $SUV_{mean} \times \text{volume}$) is indicative of asymmetric renal split function. (2) Baseline total renal PSMA uptake does not allow to infer global renal function in individual patients, but may be of value for monitoring patients at follow-up.

Our study features limitations. The study was of retrospective nature with a limited number of patients, particularly regarding patients with relevant abnormalities of split renal function and change of absolute function over time. Although the low renal excretion of [¹⁸F]-PSMA-1007 provides benefits in regard to simplified measurements of renal uptake, it does not provide a rationale to assess evaluation for obstruction, which was previously claimed to be possible with [⁶⁸Ga]-PSMA-11 [18].

Conclusion

Renal [¹⁸F]-PSMA-1007 uptake allows to detect relevant changes of renal split function with good accuracy based on a sophisticated measurement of relative unilateral total tracer uptake or a simple measurement of relative unilateral SUV_{max} . PET readers should be aware of this relationship and may report and interpret abnormalities of renal uptake accordingly.

Declarations

Funding

This study was partly funded by the 9th NAMT of the DFG, DFG-CRC1450-431460824, Münster, Germany (project B06) and a rotational clinician scientist position of the DFG-CRC1009, Münster, Germany to P.B. The other authors declare that no funds, grants, or other support were received during the preparation of this manuscript

Conflicts of interest/Competing interests

KR reports receiving consultation or lectureship fees from ABX, ABX CRO, AAA, Bayer, SIRTEX and Jansen Cielag.

Author Contributions

All authors contributed to the study conception and design. Material preparation, data collection and analysis were performed by Philipp Rassek, MD. The first draft of the manuscript was written by Philipp Rassek, MD and all authors commented on previous versions of the manuscript. All authors read and approved the final manuscript.

Data Availability

The datasets generated during and/or analysed during the current study are available from the corresponding author on reasonable request.

Code availability (software application or custom code)

Does not apply

Ethics approval (include appropriate approvals or waivers)

Analysis of clinical data has been approved by the Ethikkommission der Ärztekammer Westfalen-Lippe und der Westfälische Wilhelms-Universität Münster, No.2019-711-f-S and its later amendments).

Consent to participate (include appropriate statements)

All patients gave written informed consent for clinical [^{18}F]-PSMA-1007-PET/CT and [$^{99\text{m}}\text{Tc}$]-MAG3-scintigraphy. A formal retrospective informed consent for data analysis was not necessary.

Consent for publication

Not necessary, as no potential identifying details / images are published.

Acknowledgements

The authors thank the medical technicians and the staff of the radiochemistry group for their dedicated and reliable clinical work. The authors also thank Bernadette Riemann for data management.

References

1. Rahbar K, Afshar-Oromieh A, Jadvar H, Ahmadzadehfar H. PSMA Theranostics: Current Status and Future Directions. *Mol Imaging*. 2018;17:1536012118776068. doi:10.1177/1536012118776068
2. Backhaus P, Noto B, Avramovic N, et al. Targeting PSMA by radioligands in non-prostate disease- current status and future perspectives. *Eur J Nucl Med Mol Imaging*. 2018;45(5):860-877. doi:10.1007/s00259-017-3922-y
3. Silver DA, Pellicer I, Fair WR, Heston WD, Cordon-Cardo C. Prostate-specific membrane antigen expression in normal and malignant human tissues. *Clin Cancer Res*. 1997;3(1):81-85.
4. Delker A, Fendler WP, Kratochwil C, et al. Dosimetry for (^{177}Lu)-DKFZ-PSMA-617: a new radiopharmaceutical for the treatment of metastatic prostate cancer. *Eur J Nucl Med Mol Imaging*. 2016;43(1):42-51. doi:10.1007/s00259-015-3174-7
5. Chevalier RL. The proximal tubule is the primary target of injury and progression of kidney disease: role of the glomerulotubular junction. *Am J Physiol Renal Physiol*. 2016;311(1):F145-F161. doi:10.1152/ajprenal.00164.2016

6. Kratochwil C, Fendler WP, Eiber M, et al. EANM procedure guidelines for radionuclide therapy with ^{177}Lu -labelled PSMA-ligands (^{177}Lu -PSMA-RLT). *Eur J Nucl Med Mol Imaging*. 2019;46(12):2536-2544. doi:10.1007/s00259-019-04485-3
7. Cozzi DA, Ceccanti S, Cozzi F. Non-invasive method for assessing split renal function. *Minerva Urol Nefrol*. 2018;70(2):230. doi:10.23736/S0393-2249.18.03091-6
8. Blaufox MD, De Palma D, Taylor A, et al. The SNMMI and EANM practice guideline for renal scintigraphy in adults. *Eur J Nucl Med Mol Imaging*. 2018;45(12):2218-2228. doi:10.1007/s00259-018-4129-6
9. Rosar F, Pauly P, Ries M, et al. Determination of split renal function by PSMA imaging: comparison of ^{68}Ga -PSMA-11 PET with $^{99\text{m}}\text{Tc}$ -MAG3 scintigraphy. *Am J Nucl Med Mol Imaging*. 2020;10(5):249-256. Published 2020 Oct 15.
10. Valind K, Jögi J, Minarik D, Brolin G, Trägårdh E. Dose-reduced [^{18}F]PSMA-1007 PET is feasible for functional imaging of the renal cortex. *EJNMMI Phys*. 2021;8(1):70. Published 2021 Oct 29. doi:10.1186/s40658-021-00419-x
11. Cardinale J, Martin R, Remde Y, et al. Procedures for the GMP-Compliant Production and Quality Control of [^{18}F]PSMA-1007: A Next Generation Radiofluorinated Tracer for the Detection of Prostate Cancer. *Pharmaceuticals (Basel)*. 2017;10(4):77. Published 2017 Sep 27. doi:10.3390/ph10040077
12. Al-Adra DP, Lambadaris M, Barbas A, et al. Donor kidney volume measured by computed tomography is a strong predictor of recipient eGFR in living donor kidney transplantation. *World J Urol*. 2019;37(9):1965-1972. doi:10.1007/s00345-018-2595-x
13. Janki S, Kimenai HJAN, Dijkshoorn ML, Looman CWN, Dwarkasing RS, IJzermans JNM. Validation of Ultrasonographic Kidney Volume Measurements: A Reliable Imaging Modality. *Exp Clin Transplant*. 2018;16(1):16-22. doi:10.6002/ect.2016.0272
14. Coruh AG, Uzun C, Akkaya Z, Gulpinar B, Elhan A, Tuzuner A. Is There a Correlation with Pre-donation Kidney Volume and Renal Function in the Renal Transplant Recipient?: A Volumetric Computed Tomography Study. *Transplant Proc*. 2019;51(7):2312-2317. doi:10.1016/j.transproceed.2019.02.039
15. Werner E, Blasl C, Reiners C. Reproducibility of technetium-99m-MAG3 clearance using the Bubeck method. *J Nucl Med*. 1998;39(6):1066-1069.
16. Yamazaki T, Maruoka S, Sakamoto K. Quantification of renal function with $^{99\text{m}}\text{Tc}$ -MAG3—quantification of tubular extraction rate using Bubeck's method. *Kaku Igaku*. 1995;32(11):1199-1206.
17. Piepsz A, Tondeur M and Ham H. Relative $^{99\text{m}}\text{Tc}$ -MAG3 renal uptake: reproducibility and accuracy. *J Nucl Med* 1999; 40: 972-6.)
18. Rosar F, Pauly P, Ries M, et al. Determination of split renal function by PSMA imaging: comparison of ^{68}Ga -PSMA-11 PET with $^{99\text{m}}\text{Tc}$ -MAG3 scintigraphy. *Am J Nucl Med Mol Imaging*. 2020;10(5):249-256. Published 2020 Oct 15.

Figures

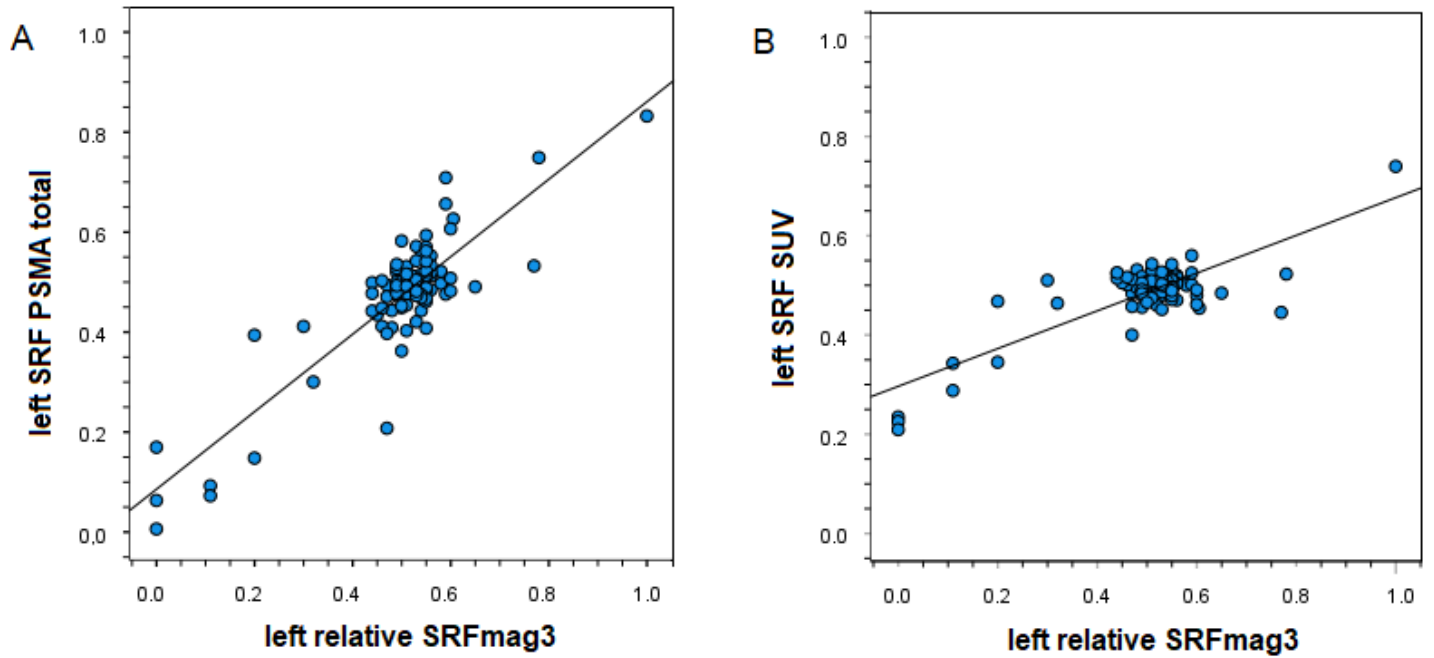


Figure 1

(A) Correlation of left $\text{SRF}_{\text{PSMA total}}$ with SRF_{MAG3} . (B) Correlation of left SRF_{SUV} with SRF_{MAG3} .

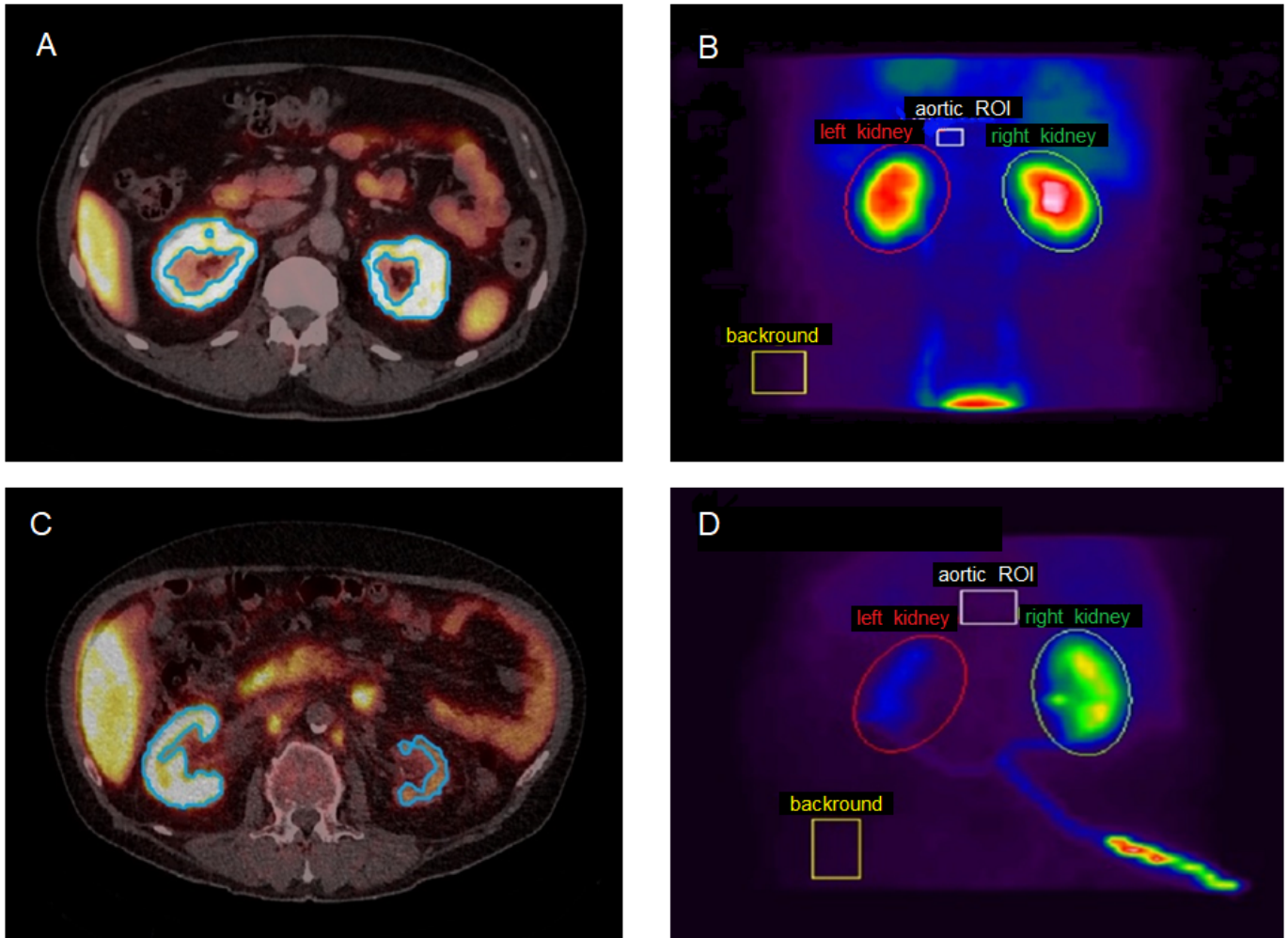


Figure 2

Representative case with symmetric SRF and TER in (A) axial fused PSMA-PET/CT (Left: SUV_{max} : 31.2, SUV_{mean} : 17.1, volume: 143 ml. Right: SUV_{max} : 31.2, SUV_{mean} : 17.9, volume: 169 ml). Images are adjusted to SUV 0-17. (B) Corresponding MAG3 scintigraphy with perfectly symmetric split function.

Representative case with abnormal split renal function both in (C) axial fused PSMA-PET/CT (Left: SUV_{max} : 13.6, SUV_{mean} : 5.8, volume 61 ml. Right: SUV_{max} : 26.1, SUV_{mean} : 14.1, volume: 243 ml). Images adjusted to SUV 0-13. (D) MAG3 scintigraphy demonstrated split renal function of left 10 % and right 90 %.

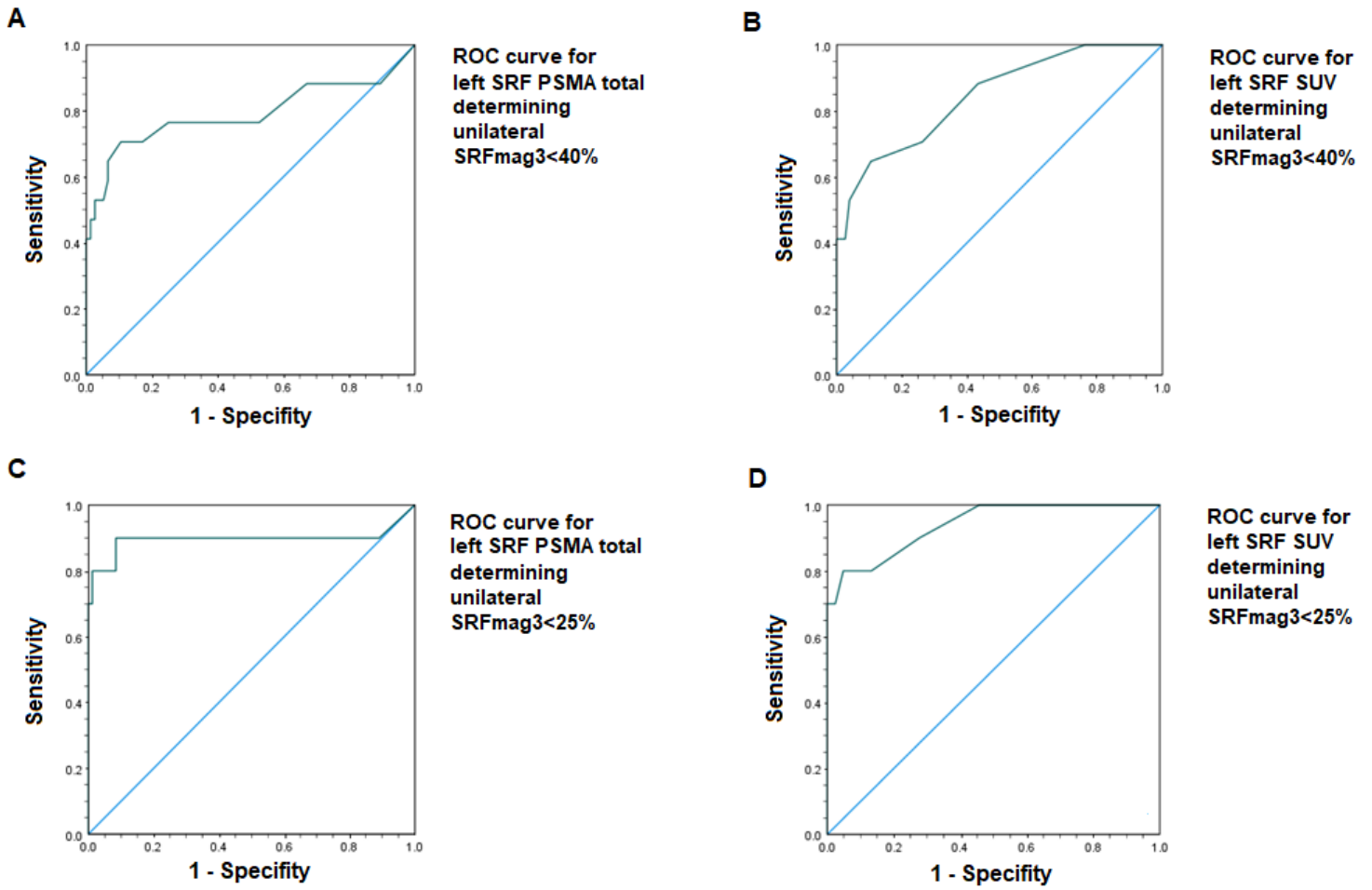


Figure 3

ROC analyses to determine any significantly abnormal uptake (Unilateral $SRF_{MAG3} < 40\%$) (A, B) and analysis for highly abnormal uptake (Unilateral $SRF_{MAG3} < 25\%$) (C, D).

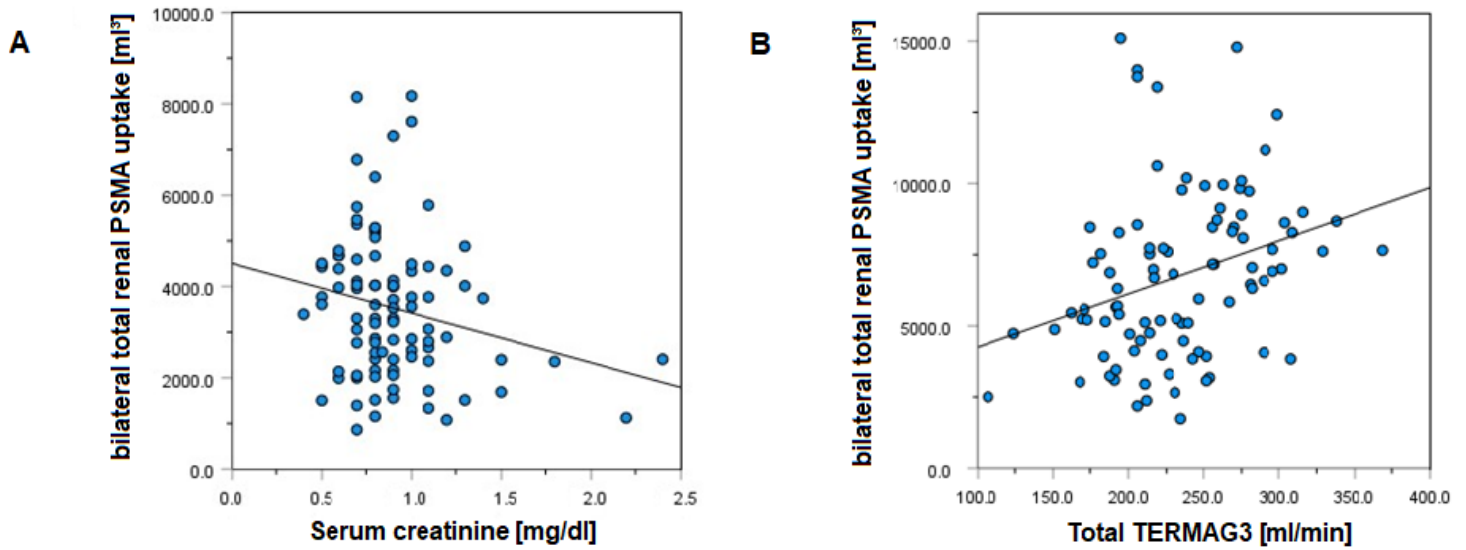


Figure 4

(A) Correlation of bilateral total renal PSMA uptake with serum creatinine and (B) TERMAG3.

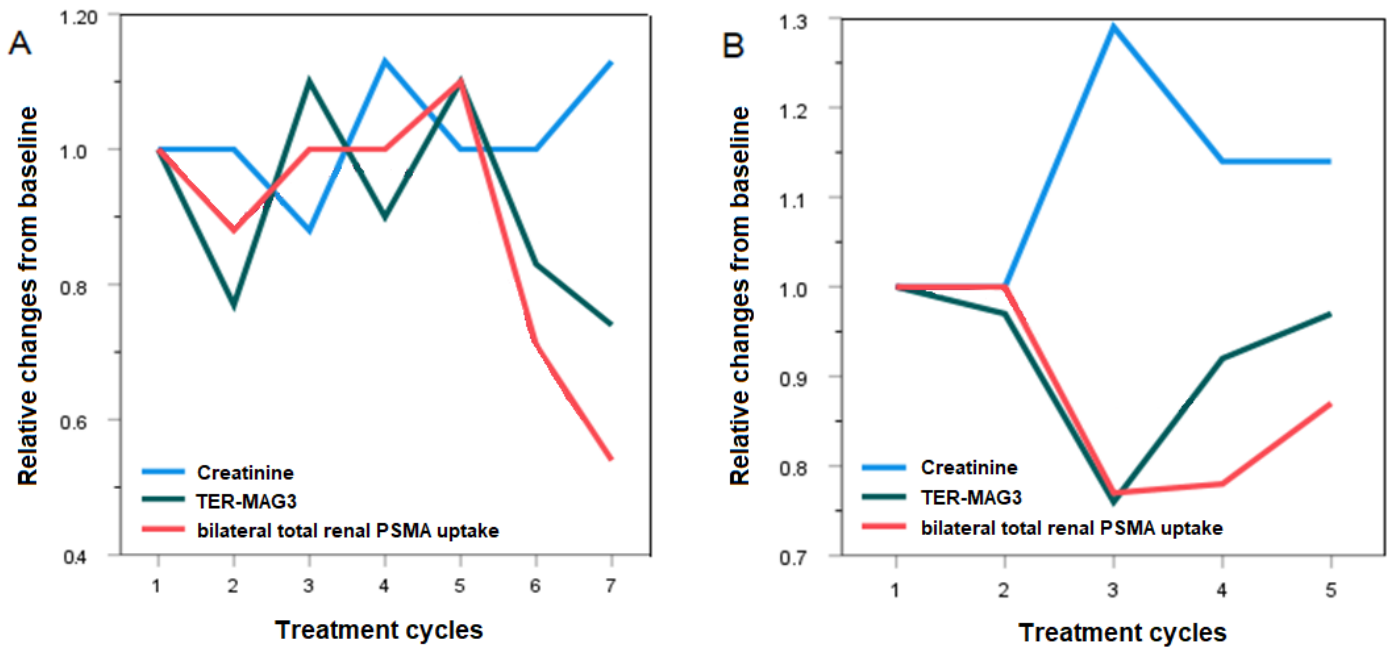


Figure 5

(A). Patient that received 7 [¹⁸F]-PSMA-1007-PET/CT and MAG3-scintigraphys at repeated cycles of radioligand therapy. Relative changes form baseline demonstrated a common trend of TER-MAG3, bilateral total renal PSMA uptake. No clear trend of creatinine is seen. (B) Patient receiving 5 [¹⁸F]-PSMA-

1007-PET/CT and MAG3-scintigraphies during repeated cycles of radioligand therapies demonstrating a common trend of TER-MAG3, bilateral total renal PMSA uptake and inversely with creatinine.